7696 *J. Phys. Chem. A* **2002,** *106,* 7696−7702

Infrared Spectra of the Novel Si_2H_2 and Si_2H_4 Species and the $SiH_{1,2,3}$ Intermediates in Solid Neon, Argon, and Deuterium

Lester Andrews* and Xuefeng Wang

Department of Chemistry, University of Virginia, P.O. Box 400319, Charlottesville, Virginia 22904-4319

Received: February 20, 2002; In Final Form: June 4, 2002

Laser-ablated silicon atoms react extensively with hydrogen to form the silicon hydrides $SiH_{1,2,3,4}$ and the disilicon hydrides $Si_2H_{2,4,6}$. Infrared spectra and density functional theory frequency calculations with HD and D_2 substitution are used to identify these species in solid neon, argon, and deuterium. The novel dibridged Si_2H_2 species is characterized by an antisymmetric Si−H−Si stretching mode at 1100.3 cm^{-1} and the trans-folded Si_2H_4 intermediate by antisymmetric SiH_2 stretching and bending modes at 2151.6 and 858.5 cm^{-1} in solid neon. The SiH_3^- anion is identified by photosensitive absorptions at 1856 and 1837 cm^{-1} in solid neon. Silicon atoms in pure deuterium gave primarily SiD_4 with some SiD_3, Si_2D_6, and Si_2D_4 and no evidence for SiD and SiD_2, but SiD_3^- and SiD_2^- were observed.

Introduction

Reactions of laser-ablated Si atoms with H_2 have been studied as part of an ongoing investigation of Ge, Sn, and Pb hydride intermediate species.[1] Silicon hydride intermediates, in the decomposition of SiH_4, particularly SiH_2 and SiH_3, are involved in the fabrication of silicon devices,[2,3] and the Si atom reaction with H_2 is also important in this regard. A large number of experimental and theoretical investigations have been performed on this system, and we will reference only those needed to support the matrix infrared identification of silicon hydride intermediate species in the reaction of laser-ablated Si atoms with H_2. These include the SiH, SiH_2, and SiH_3 transient species[4−16] and the SiH_4 and Si_2H_6 molecules.[17−20] Silicon atoms are very reactive with H_2, and the dominant product, not surprisingly, is SiH_4.

In addition, there is considerable interest in the unsaturated disilene, Si_2H_4, and disilyne, Si_2H_2, intermediate species because of their novel bonding and structures, which are different from their carbon analogues.[21−33] Silicon−silicon double bonds have been a hot topic for some time, and the current theoretical structure for Si_2H_4 is trans-bent.[27,29,31,33] Although Si_2H_4 has not been observed, the closely related CH_2SiH_2 molecule has been examined by matrix infrared and millimeter wave spectroscopy.[34,35] The Si_2H_2 ground state is a dibridged "butterfly" structure based on its submillimeter rotational spectrum from a silane, argon plasma[36] and on theoretical calculations,[21,26,28,30,33] but a slightly higher monobridged isomer has also been characterized using like methods.[37] Very recently photoionization mass spectra of Si_2H_2 and Si_2H_4 have been obtained for the transient species prepared by F atom + Si_2H_6 reactions and flash pyrolysis of Si_2H_6.[38−40] The 193 nm dissociation of disilane has also provided Si_2H_2 for observation by mass spectroscopy.[41] The SiH and SiH_2 species are expected to form Si_2H_2 and Si_2H_4 on further reactions, and we report here the first infrared spectroscopic evidence for these novel disilicon chemical species.

These laser-ablation experiments also produce and trap the stable silyl anion, SiH_3^-, which has been previously investigated in basic solution and in the gas phase.[42−45] Broad bands at 1880 and 1370 cm^{-1} have been assigned to SiH_3^- and SiD_3^- in monoglyme solution.[42] The detachment threshold of SiH_3^- has been accurately measured at 1.406 ± 0.014 eV by photoelectron spectroscopy.[45] Finally, frequencies and detachment energy have been calculated recently for the silyl anion.[33,46−48]

Experimental and Theoretical Methods

Laser-ablated silicon (RCA, 99.999%) atoms were reacted with H_2, D_2, and HD in excess neon and argon and with pure deuterium during condensation at 3.5 K using a Sumitomo Heavy Industries RDK-205D Cryocooler and methods described previously.[49,50] Infrared spectra were recorded, samples were annealed and irradiated by a mercury arc lamp, and more spectra were recorded.

Complementary density functional theory (DFT) calculations were performed using the Gaussian 98 program,[51] B3LYP and BPW91 density functionals,[52,53] and 6-311++G(d,p) basis sets[54] to provide a consistent set of vibrational frequencies for all of the silicon hydride products including mixed H, D, and all-D isotopic variants. Geometries were fully optimized, and the vibrational frequencies were computed analytically from second derivatives.

Results and Discussion

The silicon hydride matrix infrared absorptions shown in Figures 1−5 and listed in Tables 1 and 2 will be assigned on the basis of isotopic shifts, comparison with DFT computed frequencies given in Table 3, and previous theoretical and experimental investigations.

SiH. Sharp absorptions at 1971.1 (1431.4) cm^{-1} in solid neon (Figures 1 and 3) and at 1953.4 (1420.4) cm^{-1} in solid argon are assigned to the SiH (SiD) diatomic radicals. The neon frequencies are virtually the same as the gas phase[4−6] fundamentals 1970.42 (1432.86) cm^{-1} and the 17.7 cm^{-1} or 0.9% red shift for SiH to argon is reasonable.[55] Note that SiD *was not* observed in pure solid deuterium. The 1953.4 cm^{-1} band was observed but not assigned in the previous matrix isolation studies.[7,9]

---

* To whom correspondence should be addressed. E-mail: lsa@virginia.edu.

10.1021/jp0204814 CCC: \$22.00

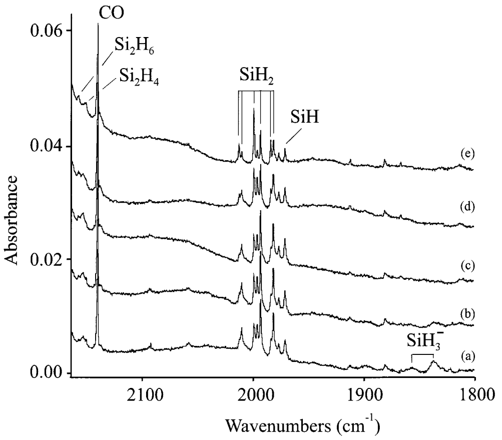

Figure 1. Infrared spectra in the 2165−1800 cm^{-1} region for laser-ablated silicon co-deposited with 10% H_2 in neon at 3.5 K: (a) sample deposited for 60 min, (b) after 290−700 nm irradiation, (c) after 240−700 nm irradiation, (d) after annealing to 7 K, and (e) after annealing to 9 K.

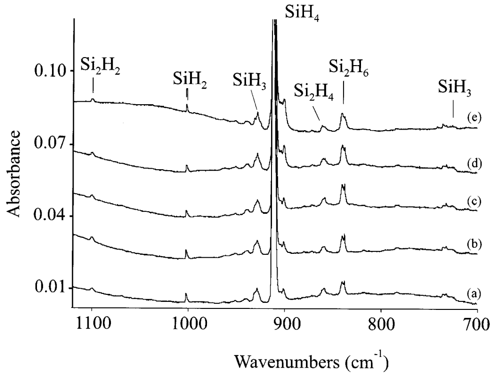

Figure 2. Infrared spectra in the 1120−700 cm^{-1} region for laser-ablated silicon co-deposited with 10% H_2 in neon at 3.5 K: (a) sample deposited for 60 min, (b) after 290−700 nm irradiation, (c) after 240−700 nm irradiation, (d) after annealing to 7 K, and (e) after annealing to 9 K.

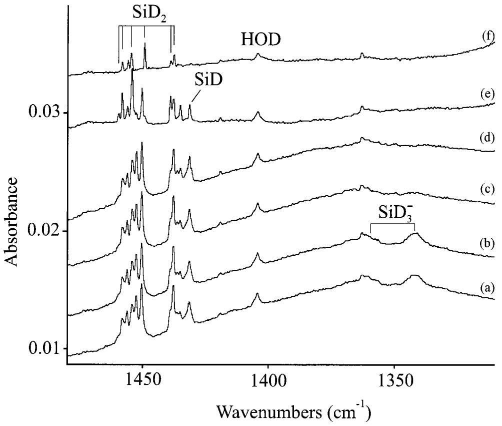

Figure 3. Infrared spectra in the 1480−1310 cm^{-1} region for laser-ablated silicon co-deposited with 5% D_2 in neon at 3.5 K: (a) sample deposited for 60 min, (b) after 380−700 nm irradiation, (c) after 290−700 nm irradiation, (d) after 240−700 nm irradiation, (e) after annealing to 10 K, and (f) after annealing to 13 K.

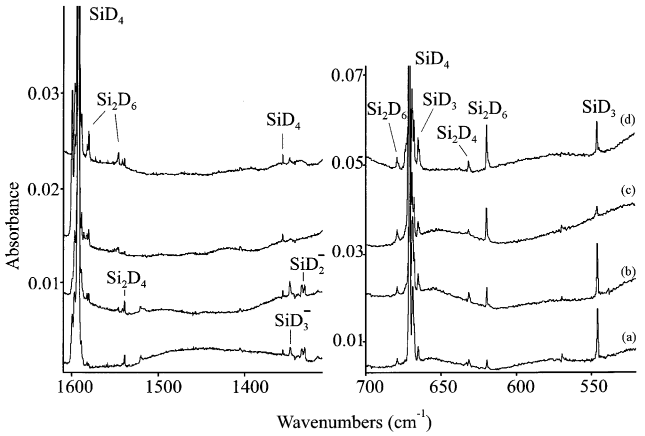

Figure 4. Infrared spectra in the 1620−1310 and 700−520 cm^{-1} regions for laser-ablated silicon co-deposited with pure deuterium at 3.5 K: (a) sample deposited for 25 min, (b) after 7 K annealing, (c) after 240−700 nm irradiation, and (d) after 8 K annealing.

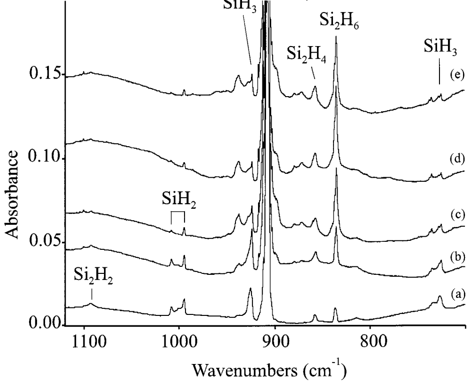

Figure 5. Infrared spectra in the 1120−700 cm^{-1} region for laser-ablated silicon co-deposited with 5% H_2 in argon at 3.5 K: (a) sample deposited for 60 min, (b) after annealing to 20 K, (c) after annealing to 26 K, (d) after 240−700 nm irradiation, and (e) after annealing to 30 K.

SiH_2. This work confirms the frequency reassignments[8] of SiH_2 (SiD_2) from earlier argon matrix spectra of silicon hydride transient species. Although the argon matrix spectra are complicated by site splittings and higher aggregate species, very good frequency agreement is found with the Rice FTIR study including the SiHD stretching modes.[8] These workers, however, assigned an 854.3 cm^{-1} bending mode[19] of SiH_2D_2 to SiHD, and we provide a new 868.5 cm^{-1} assignment for ν_2 of SiHD. The band profile for SiH_2, SiHD, and SiD_2 is identical at 1007.6 and 994.6 cm^{-1}, 879.0 and 868.5 cm^{-1}, and 728.7 and 718.6 cm^{-1}, respectively, in the bending mode region (Tables 1, 2). The same intervals are found for the sharp neon matrix counterparts at 1002.5, 875.6, and 724.8 cm^{-1} with shoulders for site splittings and for the B3LYP computed 1026.6, 894.3, and 738.2 cm^{-1} frequencies. Note that the neon matrix (875.6 cm^{-1}) and argon matrix (868.5 cm^{-1}) bending frequencies observed and 894.3 cm^{-1} frequency calculated (Table 3) for SiHD are 12.0, 11.9, and 11.9 cm^{-1}, respectively, above the median values for SiH_2 and SiD_2. Finally, the 1002.5 cm^{-1} neon matrix bending mode for SiH_2 is 3.5 cm^{-1} higher than the very recent 999.03 cm^{-1} gas-phase value.[11]

The complementary neon matrix spectra in the Si−H stretching region are interesting. The major sites on deposition at 2010.1, 1993.4, and 1981.6 cm^{-1} give way on annealing to blue-shifted sites at 2012.8, 1999.3, and 1984.1 cm^{-1} (Figure 1). The former bands are 3.1 and 4.4 cm^{-1} or 0.16 and 0.22% higher than recent gas phase observations[11] at 1978.5 and 2005.7 cm^{-1}, respectively, for ν_1 and $2\nu_2$. This suggests that the gas phase ν_3 mode for SiH_2 will occur 3−4 cm^{-1} lower than the 1993.4 cm^{-1} neon matrix value, i.e., at 1990 ± 1 cm^{-1}.

Note that SiD_2 *was not detected* in pure solid deuterium, but very strong SiD_4 and weaker SiD_3 and Si_2D_6 absorptions were

TABLE 1: Infrared Absorptions (cm^{-1}) Observed for Reactions of Laser-Ablated Silicon Atoms with Hydrogen and Deuterium

matrix	H_2	D_2	identification
Ne	2092.7	1520.7	?
D_2		1520.1	?
Ne	1971.1	1431.4	SiH, SiD
Ar	1953.4	1420.4	SiH, SiD
Ne	2012.8	1458.3	SiH_2, SiD_2: site 2, $2\nu_2$
	2010.1	1456.2	SiH_2, SiD_2: site 1, $2\nu_2$
	1999.3	1454.4	SiH_2, SiD_2: site 2, ν_3
	1993.4	1450.5	SiH_2, SiD_2: site 1, ν_3
	1984.1	1439.2	SiH_2, SiD_2: site 2, ν_1
	1981.6	1437.8	SiH_2, SiD_2: site 1, ν_1
	1002.5	724.8	SiH_2, SiD_2: site 2, ν_2
	1001.8	724.3	SiH_2, SiD_2: site 1, ν_2
Ar	1992.8	1443.6	SiH_2, SiD_2: site 1, $2\nu_2$
	1976.2		SiH_2, site 1, ν_3
	1972.8	1438.9	SiH_2, SiD_2: site 2, ν_3
	1964.9	1435.9	SiH_2, SiD_2: site 1, ν_1
	1007.6	728.7	SiH_2, SiD_2: site 2, ν_2
	994.6	718.6	SiH_2, SiD_2: site 1, ν_2
Ne	928.6	(SiD_4)	SiH_3,: ν_4
	735.4	552.3	SiH_3, SiD_3: site, ν_2
	727.3	546.2	SiH_3, SiD_3: ν_2
D_2		668.7	SiD_3: ν_4
		545.7	SiD_3: ν_2
	925.0	(SiD_4)	SiH_3: ν_4
Ar	727.2	547.2	SiH_3, SiD_3: site, ν_2
	724.9	545.4	SiH_3, SiD_3: ν_2
Ne	2191.8	1599.3	SiH_4, SiD_4: ν_3
	1880.4	1363.0	SiH_4, SiD_4: $\nu_2 + \nu_4$
	913.2	674.2	SiH_4, SiD_4: ν_4
D_2		1593.2	SiD_4: ν_3
		1355.6	SiD_4: $\nu_2 + \nu_4$
		670.9	SiH_4, SiD_4: ν_4
Ar	2176.8	1588.9	SiH_4, SiD_4: ν_3
	905.3	668.7	SiH_4, SiD_4: ν_4
Ne	2172	1585	Si_2H_6, Si_2D_6: ν_7
	2158	1551	Si_2H_6, Si_2D_6: ν_5
	840.8	622.5	Si_2H_6, Si_2D_6: ν_6
D_2		1580.6	Si_2D_6: ν_7
		1546.0	Si_2D_6: ν_5
		679.0	Si_2D_6:ν_8
		619.6	Si_2D_6: ν_6
Ar	835.2	618.0	Si_2H_6, Si_2D_6: ν_6
Ne	1856	1357	SiH_3^-, SiD_3^-: ν_1
	1837	1342	SiH_3^-, SiD_3^-: ν_3
Ne	1823	1330	SiH_2^-, SiD_2^-
D_2		1333.4	SiD_2^-
		1330.4	SiD_2^-
Ne	1100.3	823.7	Si_2H_2, Si_2D_2
Ar	1093.3	815.0	Si_2H_2, Si_2D_2
Ne	2154.0	1560.2	Si_2H_4, Si_2D_4 site
	2151.6	1558.4	Si_2H_4, Si_2D_4
	861.4	634.2	Si_2H_4, Si_2D_4 site
	858.5	632.0	Si_2H_4, Si_2D_4
D_2		1539.1	Si_2D_4
		631.6	Si_2D_4
Ar	2150.5		Si_2H_4
	2145.5		Si_2H_4 site
	857.3	630.7	Si_2H_4, Si_2D_4

TABLE 2: Infrared Absorptions (cm^{-1}) Observed for Reactions of Laser-Ablated Silicon Atoms with HD

matrix	HD	identification
Ne	2092.5, 1520.7	?
Ne	1971.1, 1431.4	SiH, SiD
Ar	1953.4, 1420.4	SiH, SiD
Ne	1999.7, 1452.7	SiHD: site 2
	1993.8, 1449.0	SiHD: site 1
	875.6	SiHD: site 2
	874.9	SiHD: site 1
Ar	1975.8, 1437.4	SiHD
	879.0	SiHD: site ν_2
	868.5	SiHD: ν_2
Ne	−, 602.9	SiH_2D, $SiHD_2$: site
	668.5, 600.9	SiH_2D, $SiHD_2$
Ne	1844, 1837	SiH_2D^-, $SiHD_2^-$
	1350, 1342	SiH_2D^-, $SiHD_2^-$
Ne	1077.8	Si_2HD
Ne	769.6	SiHDSiHD site
	767.7	SiHDSiHD site
Ar	767.4	SiHDSiHD site

observed (Figure 4). Apparently, the laser-ablated Si atom reaction gives SiD_2, which reacts rapidly to form SiD_4. Such is not the case for Ge as GeD_2 is observed in pure solid deuterium.[1]

SiH_3. The SiH_3 radical has been characterized by numerous gas-phase investigations[13−16] after it was first observed by matrix ESR methods[12] and tentatively assigned incorrectly in matrix infrared spectra of silicon hydride intermediates.[7,9] The SiH_3 radical is not a major product here, but it is clearly identified from the ν_2 mode in a clear region of the spectrum. A weak 725.4 cm^{-1} neon matrix absorption and 727.2 and 724.9 cm^{-1} argon matrix bands are so assigned based on agreement with the gas-phase spectrum (inversion split transitions 721.0 and 727.9 cm^{-1}).[13,14] We observed a higher yield of SiD_3 site split at 552.3 and 546.2 cm^{-1} in solid neon (Figure 3), 547.2 and 545.4 cm^{-1} in solid argon, and a still larger yield in pure deuterium as a single sharp 545.7 cm^{-1} absorption. The latter is in excellent agreement with the recent assignment of a sharp 545.8 cm^{-1} band following H_2 resonance photolysis of SiD_4 in solid D_2 by the Weltner group.[20] Our neon matrix experiment with Si and HD instead produced new similar shaped bands at 668.5 and 600.9 cm^{-1}, which are in the proper intermediate position, based on B3LYP isotopic frequency calculations, for this mode of the SiH_2D and $SiHD_2$ radicals.

In solid D_2, the SiD_3 band at 545.7 cm^{-1} is markedly reduced by broadband photolysis but almost restored on annealing. A sharp 668.7 cm^{-1} band behaves in like fashion and is appropriate for ν_4 of SiD_3. Our solid argon experiment with H_2 reveals a new 925.0 cm^{-1} band, which sharpens to 923.9 cm^{-1} on annealing and tracks with the 727.2 and 724.9 cm^{-1} SiH_3 bands, and this band can be assigned to ν_4 of SiH_3. The neon matrix counterpart is 928.6 cm^{-1}. The DFT frequency calculations in Table 3 support these vibrational assignments to SiH_3. Previous matrix experiments observed and assigned the 925 cm^{-1} band, and the discharge work reported, but did not assign the 727 cm^{-1} absorption.[7,9] Finally, we fail to observe the ν_3 mode of SiH_3, reported at 2185.2 cm^{-1} in the gas phase,[16] owing to masking by the red wing of the SiH_4 absorption.

SiH_4. Silane is produced here as the major reaction product, as expected. The strong SiH_4 and SiD_4 fundamental bands in solid argon are in ±0.2 cm^{-1} agreement with the Florida group[20] and the neon matrix bands agree ±0.3 cm^{-1} with the Texas Tech group[19] using the authentic materials. Likewise the SiD_4 fundamentals produced here from Si co-deposited with pure deuterium are in ±0.2 cm^{-1} agreement with the Weltner group[20] measurements for SiD_4 in D_2 at 4 K. Finally, the neon matrix fundamentals of SiH_4 and SiD_4 are blue shifted from the argon matrix values and very near (±1 cm^{-1}) the gas-phase values.[17]

Si_2H_6. Disilane is observed here from SiH_3 dimerization or possibly reaction of SiH_2 and SiH_4. The argon matrix band positions (Table 1) agree with those of previous workers,[7,9] and the slightly blue-shifted neon matrix measurements are very close to the gas-phase value.[18] Finally, sharp, weak bands appear at 879.2, 871.9, and 735.0 cm^{-1} on annealing to 26 K in solid argon after Si_2H_6 absorption is appreciable at 835.1 cm^{-1}. These much weaker absorptions are probably due to higher hydrides such as Si_3H_8. Similar weak bands are observed in solid neon at 879.5, 871.8, and 735.7 cm^{-1} (Figure 1).

TABLE 3: Frequencies (cm^{-1}), Infrared Intensities (km/mol), Bond Lengths, and Angles Calculated at the B3LYP/6-311++G(d,p) Level for Silicon Hydrides

SiH	2007.3 (347)	SiD	1444.3 (180)				
$^2\Pi$							
1.534 Å							
SiH_2	2036.6 (293)	SiHD	2036.1 (303)	SiD_2	1465.5 (160)		
$^1A_1$	2035.8 (310)		1464.7 (159)		1463.9 (160)		
(C_{2v})	1026.6 (113)		894.3 (85)		738.2 (56)		
1.527 Å, 91.5°							
SiH_3	2240.1 (132 × 2)	SiH_2D	2240.0 (133)	$SiHD_2$	2227.0 (95)	SiD_3	1585.6 (65 × 2)
$^2A_1$	2199.1 (8)		2213.4 (53)		1620.7 (74)		1523.9 (4)
(C_{3v})	937.2 (70 × 2)		1600.5 (49)		1580.7 (25)		650.8 (30 × 2)
1.486 Å, 111.2°	760.8 (80)		927.0 (69)		844.2 (56)		530.0 (33)
			787.8 (49)		707.6 (44)		
			696.7 (69)		617.9 (49)		
SiH_4	2245.3 (126 × 3)	SiH_2D_2	2245.1 (128)	SiD_4	1622.4 (76 × 3)		
$^1A_1$	2237.5 (0)		2241.4 (66)		1582.7 (0)		
(T_d)	979.3 (0)		1622.5 (74)		692.8 (0)		
1.484 Å	921.1 (152 × 3)		1602.6 (35)		676.8 (80)		
			951.2 (68)				
			865.8 (132)				
			848.2 (0)				
			746.5 (100)				
			684.2 (47)				
Si_2H_6	2232.1 (215 × 2)	Si_2D_6	1613.4 (121 × 2)				
$^1A_{1g}$	2222.5 (0 × 2)		1605.2 (0 × 2)				
(D_{3d})	2222.2 (0)		1581.8 (0)				
1.487 Å	2213.5 (124)		1574.3 (73)				
Si−Si−H: 110.4°	960.1 (91 × 2)		695.1 (0)				
	946.0 (0 × 2)		689.1 (47 × 2)				
	928.6 (0)		675.7 (0 × 2)				
	855.4 (548)		630.4 (296)				
	637.2 (0 × 2)		484.8 (0 × 2)				
	422.6 (0)		397.0 (0)				
	382.0 (27 × 2)		273.0 (14 × 2)				
	136.4 (0)		96.5 (0)				
SiH^-	1820.6 (830)	SiD^-	1310.8 (399)				
$^3\Sigma^-$							
1.562 Å							
SiH_2^-	1857.6 (816)	$SiHD^-$	1855.4 (764)	SiD_2^-	1334.6 (337)		
$^2B_1$	1853.5 (703)		1334.6 (370)		1334.3 (410)		
(C_{2v})	963.1 (170)		839.3 (120)		693.0 (71)		
1.554 Å, 92.4°							
SiH_3^-	1900.9 (660)	SiH_2D^-	1896.6 (670)	$SiHD_2^-$	1892.7 (678)	SiD_3^-	1361.1 (331 × 2)
$^1A_1$	1889.3 (676 × 2)		1889.3 (678)		1361.1 (331)		1359.7 (335)
(C_{3v})	956.6 (59 × 2)		1361.4 (327)		1360.9 (329)		683.4 (23 × 2)
1.546 Å,	868.4 (205		938.5 (77)		837.4 (42)		636.4 (87)
95.0°			825.1 (39)		782.8 (92)		
			779.3 (142)		663.3 (62)		
SiH^+	2129.1 (73)	SiD^+	1532.0 (47)				
$^1\Sigma^+$							
1.519 Å							
SiH_2^+	2231.3 (b_2, 1)	$SiHD^+$	2191.8 (2)	SiD_2^+	1618.1 (0)		
$^2A_1$	2146.5 (a_1, 4)		1571.9 (1)		1531.4 (1)		
(C_{2v})	906.0 (a_1, 40)		791.1 (35)		656.4 (25)		
1.492 Å,							
119.5°							
Si_2H_2[a]	1612.9 (a_1, 5)	Si_2HD	1566.9 (10)	Si_2D_2	1147.7 (3)		
$^1A_1$	1530.0 (b_1, 10)		1132.1 (3)		1093.9 (5)		
2.219 Å	1168.3 (b_2, 381)		1127.9 (224)		847.3 (200)		
1.681 Å	1076.4 (a_2, 0)		837.8 (35)		771.7 (0)		
SiHSi:	960.2 (a_1, 47)		804.1 (66)		710.6 (22)		
82.6°	523.0 (a_1, 1)		517.3 (1)		505.5 (3)		
Si_2H_4	2264.0 (b_u, 151)	SiHDSiHD	2250.0 (79)	Si_2D_4	1638.5 (85)		
^1A_g	2252.1 (b_g, 0)		2241.8 (56)		1629.3 (0)		
(C_{2h})	2235.4 (a_g, 0)		1619.1 (37)		1600.2 (0)		
2.174 Å	2231.1 (b_u, 113)		1611.7 (32)		1594.4 (63)		
1.483 Å	995.7 (a_g, 0)		845.1 (2)		713.0 (0)		
118.7°	919.4 (b_u, 181)		818.4 (129)		665.0 (94)		
112.1°	615.8 (b_g, 0)						
	560.9 (a_g, 0)						
	524.3 (a_u, 0)						
	446.9 (b_u, 32)						
	347.6 (a_u, 22)						
	324.9 (a_g, 0)						

[a] The $^3B_{1u}$ state (D_{2h} symmetry) is 40.7 kcal/mol higher with very strong 1357.2 cm^{-1} (b_{1u}, 1525 km/mol) mode.

Si_2H_2. The neon matrix experiments with H_2 reveal a new 1100.3 cm^{-1} absorption (Figure 2) which shifts to 823.7 cm^{-1} with D_2 and to 1077.8 cm^{-1} with HD. This band falls above SiH_2 bending modes, and below Si−H stretching modes, but in the region predicted for bridged Si−H−Si antisymmetric stretching modes.[30] This is in accord with the lower H/D ratio (1.336) for a more anharmonic vibration. We recalculated frequencies for both the ground state dibridged and the slightly higher energy monobridged isomer to obtain mixed Si_2HD isotopic frequencies on a consistent scale with the other product species. The lower energy dibridged isomer has one Si_2HD isotopic form with strong (essentially Si−H−Si) frequency 12.6% of the way down from Si_2H_2 to Si_2D_2, which is in reasonable agreement with our observation. The monobridged isomer, however, has two mixed isotopic modifications with little (6 cm^{-1}) shift computed for D(Si_2H), which is not in agreement with our spectrum. Hence, the 1100.3 cm^{-1} band and 1093.0 cm^{-1} argon matrix counterpart are assigned to Si_2H_2 with the novel dibridged structure. The earlier theoretical investigation[30] also incorporated anharmonic corrections and predicted the very strong Si_2H_2 fundamental at 1092 cm^{-1}, which provides strong support for our matrix infrared identification of Si_2H_2. The earlier and present calculations find the b_2 antisymmetric stretching mode stronger by an order of magnitude than other modes. Hence, this infrared detection of Si_2H_2 rests on one fundamental. Gas-phase diode laser spectroscopy should locate Si_2H_2 near 1100 cm^{-1}.

Si_2H_4. Another SiH_2 bending mode absorption is observed between the strongest bending absorptions for SiH_4 and Si_2H_6. This new band appears at 858.5 (632.0) cm^{-1} for H_2(D_2) in neon (Figure 2), at 857.3 (630.7) cm^{-1} in argon (Figure 5), and at 631.6 cm^{-1} in pure deuterium (Figure 4). The neon and argon matrix bands were characterized by a distinct doublet split band contour, which enabled the association of like contour 2154.0 (1560.2) cm^{-1} absorptions in the Si−H(D) stretching region. Note the annealing behavior of these new bands and Si_2H_6 in neon where the new bands decreased slightly, whereas Si_2H_6 increased slightly (Figures 1 and 2).

Our B3LYP calculation finds the same C_{2h} structure for the ground-state Si_2H_4 molecule as a recent theoretical investigation[33] and, in addition, predicts the strongest infrared absorption of Si_2H_4 to be a bending mode at 919.4 cm^{-1}, which is between the strong bending modes computed for SiH_4 and Si_2H_6 and 7% higher than the observed 858.5 cm^{-1} band. Of perhaps more importance, our calculation predicts the strongest bending mode for SiHDSiHD to be 39.7% of the shift from Si_2H_4 to Si_2D_4, and the observed band at 769.6 cm^{-1} is 39.2% of the deuterium shift, which strongly supports our assignment.

The two b_u Si−H stretching modes should be observable, but the higher one is computed near the ν_3 mode for SiH_4 and will be covered in these experiments. However, the other b_u mode is predicted 14 cm^{-1} lower than SiH_4, and the observed 2154.0 cm^{-1} band is below SiH_4 by 38 cm^{-1} and in reasonable agreement. The split 2154.0 and 2151.6 cm^{-1} band absorbance (0.001) is half of that for the split 861.4 and 858.5 cm^{-1} band (0.002) in agreement with the relative calculated intensities. Note the slight growth of Si_2H_6 at 2158 cm^{-1} and decrease of Si_2H_4 bands at 2154.0 and 2151.6 cm^{-1} on annealing. Note also reversal of the two matrix site bands at 861.4 and 858.5 cm^{-1} and at 2154.0 and 2151.6 cm^{-1} on annealing, which helps to associate these absorptions with the same molecular species.

The 631.6 cm^{-1} band in pure deuterium decreases on photolysis, whereas the 619.6 cm^{-1} Si_2D_6 band increases, but subsequent annealing to 8 K restores the 631.6 cm^{-1} absorption and further increases Si_2D_6. A sharp 1539.1 cm^{-1} band exhibits identical photolysis and annealing behavior with the 631.6 cm^{-1} band and is half as intense; this behavior is repeated in another photolysis/annealing cycle. The 1539.1 cm^{-1} band is assigned to the lower b_u stretching mode of Si_2D_4 in pure deuterium, and the upper b_u mode is masked by SiD_4.

This work reports the first absorption spectroscopic evidence for the trans-folded Si_2H_4 intermediate predicted by theory to have a different structure than C_2H_4.[27,29,31,33]

SiH_3^-. New absorptions at 1856 and 1837 cm^{-1} are characterized by their photodestruction. In fact, these bands are 70% destroyed by 290−700 nm photolysis (Figure 1). Furthermore, these absorptions do not appear in an identical experiment with 0.1% CCl_4 added to the neon, 10% H_2 reagent to serve as an electron trap;[56−58] hence, a molecular anion must be considered. Our 1856 and 1837 cm^{-1} neon matrix absorptions fall between the 1885 and 1880 cm^{-1} Raman and IR measurements for SiH_3^- in solution[42] and recent anharmonic calculations of 1843 and 1819 cm^{-1} for the ν_1 and ν_3 modes of the gaseous SiH_3^- anion.[47] This agreement is compelling and indicates a like assignment for our neon matrix bands. On the basis of the near agreement of gaseous and neon matrix SiH_2 and SiH_4 stretching fundamentals, we predict ν_3 of SiH_3^- in the gas phase at 1837 ± 5 cm^{-1}.

The SiH_3^- assignment is supported by deuterium substitution, which produces similar 1357 and 1342 absorptions for SiD_3^- in neon (H/D ratios 1.368 and 1.369) and at 1347.5 cm^{-1} in pure deuterium. The spectra in Figure 3 show that these bands are virtually destroyed by 290−700 nm photolysis. In our HD experiment, which produces SiH_2D^- and $SiHD_2^-$ anions, the bands are broadened to the blue from the pure isotopic positions giving 1844 and 1350 cm^{-1} shoulders. Our DFT calculations predict the strongest absorptions for SiH_2D^- and $SiHD_2^-$ to be common with SiH_3^- and SiD_3^-, respectively, but because the symmetric stretching mode is higher, symmetric stretching modes for SiH_2D^- and $SiHD_2^-$ fall higher than the antisymmetric stretching modes as well, and the above blue shoulders are due to such modes.

The SiH_3^- absorption was substantially reduced by $\lambda > 290$ nm radiation, which is in excess of the photodetachment energy threshold.[45] Such is typically the case for matrix-isolated molecular anions and broadband radiation. The recently computed adiabatic and zero-point corrected adiabatic electron affinities[33] for SiH_3 are in excellent agreement with the experimental value.[45] Our B3LYP SiH_3^- − SiH_3 energy difference (31.6 kcal/mol) is in good agreement with these values as well.

SiH_2^-. A very weak 1823 cm^{-1} band and 1330 cm^{-1} D_2 counterpart show the same photolysis and CCl_4 doping and behavior as described for the SiH_3^- bands, so another anion must be considered. The H/D = 1.371 ratio is appropriate for an Si−H(D) stretching mode. Our B3LYP calculations predict the strongest infrared absorption for SiH_2^- about 30 cm^{-1} below that for SiH_3^- and the 1823 cm^{-1} band is in reasonable agreement. The SiH_2^- anion has also been observed in the gas phase[59] with a slightly lower detachment threshold than SiH_3^-.

The pure deuterium experiment reveals two photosensitive bands at 1333.4 and 1330.4 cm^{-1}, which are just below the 1347.5 cm^{-1} band assigned above to SiD_3^- in pure deuterium. The former deuterium matrix bands are stronger than the 1330 cm^{-1} neon matrix absorption and make a better case for infrared identification of SiD_2^-. Although SiD_2 was not observed in pure solid deuterium, SiD_2^- appears to be stable in this medium.

Apparently, there is no driving force for reaction with D_2 to give the unstable SiD_4^- anion.[33]

Other Absorptions. Sharp weak bands at 2092.7 (1520.7) cm^{-1} in solid neon decrease in concert with SiH_3^- on photobleaching. The H/D ratio (1.376) is appropriate for an Si−H(D) vibration, and the proximity to the 2088.7 cm^{-1} fundamental of SiH^+ in the gas phase[60] raises this possible assignment. However, a similar 1520.1 cm^{-1} feature is observed in pure deuterium, and we believe SiD^+ should react to form SiD_3^+ in pure deuterium. Ionizing radiation is produced in the laser-ablation process as attested by the observation of Ar_nD^+ at 643.1 cm^{-1} in the argon matrix experiments.[61] SiH_2^+(SiD_2^+) is a possiblilty,[62] but the low infrared intensity (Table 3) and HD observation cast doubt. This weak photosensitive absorption remains unassigned.

The very weak absorption at 1912.3 cm^{-1} increased on annealing in solid neon (Figure 1) and is unshifted with D_2. This peak is 14.2 cm^{-1} above SiCO in solid argon[63] and is probably due to SiCO made by the Si atom reaction with CO impurity.

Reaction Mechanisms. In a reverse of the SiH_4 chemical vapor deposition process, silicon atoms react extensively with hydrogen. The primary reaction 1 of Si and H_2 to give SiH is endothermic (+32.7 kcal/mol),[60] where laser-ablated Si contains sufficient excess energy[64] to drive the reaction, and reaction 2 to give the SiH_2 intermediate is exothermic (B3LYP, −40.9 kcal/mol). The spontaneous nature of reaction 2 is demonstrated by the formation of SiH_2 using less-energetic thermal ground-state Si atoms.[8] Laser-ablation probably produces excited ^1D (+18.0 kcal/mol) as well as ground state ^3P Si atoms although collisions with matrix atoms during condensation are expected to relax most of the excited Si atoms. Reaction 2 likely first forms $SiH_2(^3B_1)$, which is +18 or 21 kcal/mol higher than $SiH_2(^1A_1)$,[65] but this intermediate step is −23 or −20 kcal/mol exothermic, and the triplet intermediate is relaxed by the matrix. A minor amount of SiH_2 is made by highly exothermic (B3LYP, −73.6 kcal/mol) reaction 3 based on the observation of small amounts of SiHD in the $H_2 + D_2$ and SiH_2 and SiD_2 in the HD experiments. The presence of H(D) atoms in these experiments is attested by the detection of $HO_2(DO_2)$.[66]

$$Si(^3P) + H_2(^1\Sigma_g^+) \rightarrow SiH(^2\Pi) + H(^2S) \quad (1)$$

$$Si(^3P) + H_2(^1\Sigma_g^+) \rightarrow [SiH_2(^3B_1)] \xrightarrow{relax} SiH_2(^1A_1) \quad (2)$$

$$SiH + H \rightarrow SiH_2 \quad (3)$$

The major secondary reaction 4 accounts for the formation of SiH_4, which is also considerably exothermic (B3LYP, −53.1 kcal/mol). This reaction is spontaneous based on the growth of SiH_4 on annealing to 16−20 K in solid argon.

Our HD experiment, however, reveals about 20% as much SiH_3D and $SiHD_3$ as SiH_2D_2 absorption intensity, which indicates that exothermic H atom reactions are involved, as must be the case for SiH_3 radical formation. Reactions 5 and 6 are highly exothermic (B3LYP, −68.4 and −87.6 kcal/mol, respectively):

$$SiH_2 + H_2 \rightarrow SiH_4 \quad (4)$$

$$SiH_2 + H \rightarrow SiH_3 \quad (5)$$

$$SiH_3 + H \rightarrow SiH_4 \quad (6)$$

The silyl anion, SiH_3^-, is formed by the exothermic (B3LYP, −31.6 kcal/mol) capture by the silyl radical of electrons produced in the ablation process. The SiH_2^- anion is made in like fashion (exothermic, B3LYP, −27.2 kcal/mol). Doping with CCl_4 preferentially captured ablated electrons[56−58] and prevented the formation of these product anions.

$$SiH_3 + e^- \rightarrow SiH_3^- \quad (7)$$

$$SiH_2 + e^- \rightarrow SiH_2^- \quad (8)$$

The butterfly-shaped Si_2H_2 species can be formed by further Si reaction with SiH_2 or by the dimerization of SiH, which are both highly exothermic (B3LYP, −69.1 and −72.0 kcal/mol, respectively). The dimerizations of SiH_2 and SiH_3 are less exothermic (B3LYP, −55.3 and −44.2 kcal/mol, respectively). The Ge_2H_2 species[1] is formed mostly by the analogue of reaction 9. Although this reaction is spin forbidden, it proceeds in the collision-rich matrix environment[67] probably through a $Si_2H_2(^3B_{1u})$ state. Formation of this triplet intermediate state is −28.4 kcal/mol exothermic, and the subsequent relaxation process is −40.7 kcal/mol exothermic. These experiments provide the first vibrational spectroscopic evidence for the novel Si_2H_2 and Si_2H_4 species:

$$SiH_2(^1A_1) + Si(^3P) \rightarrow [Si_2H_2(^3B_{1u})] \xrightarrow{relax} Si_2H_2(^1A_1) \quad (9)$$

$$SiH + SiH \rightarrow Si_2H_2(^1A_1) \quad (10)$$

$$SiH_2 + SiH_2 \rightarrow Si_2H_4(C_{2h}) \quad (11)$$

$$SiH_3 + SiH_3 \rightarrow Si_2H_6(D_{3d}) \quad (12)$$

The reactions of silicon atoms in pure deuterium are noteworthy. The major product is SiD_4 as expected (Figure 4). The next strongest signals are due to SiD_3 and Si_2D_6. More growth on annealing and photolysis is observed for Si_2D_6 than SiD_4. The SiD_3 radical and Si_2D_4 are decreased substantially by ultraviolet photolysis. One interesting observation is the partial restoration of SiD_3 and Si_2D_4 on 8 K annealing: this suggests that some unreacted Si and D atoms are present in solid D_2 at 3.5 K, and more reactions occur on diffusion in solid deuterium at 8 K. As SiD is not observed when formed, SiD probably rapidly undergoes exothermic (−38.5 kcal/mol) reaction 13. The implication is that the Si reaction with D_2 may require a small activation energy. A likely route for the reformation of Si_2D_4 is the Si atom reaction with SiD_4, which is a highly exothermic reaction (−93.3 kcal/mol):

$$Si + D + D_2 \rightarrow SiD + D_2 \rightarrow SiD_3 \quad (13)$$

$$Si + SiD_4 \rightarrow Si_2D_4 \quad (14)$$

In addition there is evidence for the trapping of SiD_2^- in solid deuterium, whereas SiD_2 is not observed. Because SiD_2^- is a stable anion and SiD_4^- is not stable,[33] SiD_2^- is not expected to react with D_2 like SiD_2 clearly does to form SiD_4.

Conclusions

Laser-ablated silicon atoms react extensively with molecular hydrogen to form the silicon hydrides $SiH_{1,2,3,4}$ and the disilicon hydrides $Si_2H_{2,4,6}$. Infrared spectra and density functional theory frequency calculations with HD and D_2 substitution are used to identify these species in solid neon, argon, and deuterium matrix samples. The novel dibridged Si_2H_2 disilyne is characterized by an antisymmetric Si−H−Si stretching mode at 1100.3 cm^{-1}, and the trans-folded Si_2H_4 disilene is characterized by antisymmetric SiH_2 stretching and bending modes at 2151.6 and 858.5 cm^{-1} in solid neon. The SiH_3^- anion is identified by photosensitive absorptions at 1856 and 1837 cm^{-1} in solid neon. Silicon atoms in pure deuterium gave primarily SiD_4 with some SiD_3, Si_2D_6, and Si_2D_4, weak SiD_3^- and SiD_2^-, but no evidence for SiD and SiD_2.

Acknowledgment. We gratefully acknowledge support for this work from N.S.F. Grant CHE 00-78836.

References and Notes

(1) Wang, X.; Andrews, L.; Kushto, G. P. *J. Phys. Chem. A* **2002**, *106*, 5809. Wang, X.; Andrews, L. *J. Phys. Chem. A* **2002**, *106*, 6302.

(2) Jasinski, J. M.; Gates, S. M. *Acct. Chem. Res.* **1991**, *24*, 9.

(3) Kessels, W. M. M.; Bougaarts, M. G. H.; Hoefragels, J. P. M.; Sihram, D. C.; van de Sander, M. C. M. *J. Vac. Sci. Technol.* **2001**, *19*, 1027.

(4) Knights, J. C.; Schmitt, J. P. M.; Perrin, J.; Guelachvili, G. *J. Chem. Phys.* **1982**, *76*, 3414.

(5) Davies, P. B.; Isaacs, N. A.; Johnson, S. A.; Russell, D. K. *J. Chem. Phys.* **1985**, *83*, 2060.

(6) Betrencourt, M.; Boudjaadar, D.; Chollet, P.; Guelachvili, G.; Morillon-Chapey, M. *J. Chem. Phys.* **1986**, *84*, 4121.

(7) Milligan, D. E.; Jacox, M. E. *J. Chem. Phys.* **1970**, *52*, 2594.

(8) Fredin, L.; Hauge, R. H.; Kafafi, Z. H.; Margrave, J. L. *J. Chem. Phys.* **1985**, *82*, 3542.

(9) Lloret, A.; Abouaf-Marguin, L. *Chem. Phys.* **1986**, *107*, 139.

(10) Yamada, C.; Kanamori, H.; Hirota, E.; Nishiwaki, N.; Itabashi, N.; Kato, K.; Goto, T. *J. Chem. Phys.* **1989**, *91*, 4582.

(11) Ishikawa, H.; Kajimoto, O. *J. Mol. Spectrosc.* **1991**, *150*, 610; **1993**, *160*, 1; **1995**, *174*, 270.

(12) Jackel, G. S.; Christiansen, J.; Gordy, W. *J. Chem. Phys.* **1967**, *47*, 4274.

(13) Yamada, C.; Hirota, E. *Phys. Rev. Lett.* **1986**, *56*, 923.

(14) Johnson, R. D., III.; Tsai, B. P.; Hudgens, J. W. *J Chem. Phys.* **1989**, *91*, 3340.

(15) Quandt, R. W.; Hershberger, J. F. *Chem. Phys. Lett.* **1993**, *206*, 355.

(16) Sumiyoshi, Y.; Tanaka, K.; Tanaka, T. *Appl. Surf. Sci.* **1994**, *79/80*, 471.

(17) Meal, J. H.; Wilson, M. K. *J. Chem. Phys.* **1956**, *24*, 385.

(18) Bethke, G. W.; Wilson, M. K. *J. Chem. Phys.* **1957**, *26*, 1107.

(19) Wilde, R. E.; Srinivasan, T. K. K.; Harral, R. W.; Sankar, S. G. *J. Chem. Phys.* **1971**, *55*, 5681.

(20) Li, L.; Graham, J. T.; Weltner, W., Jr. *J. Phys. Chem. A.* **2001**, *105*, 11018.

(21) Lischka, H.; Köhler, H. *J. Am. Chem. Soc.* **1983**, *105*, 6646.

(22) Allen, W. D.; Schaefer, H. F., III. *Chem. Phys.* **1986**, *108*, 243. West, R. *Angew. Chem., Int. Ed. Engl.* **1987**, *26*, 1201.

(23) Trinquier, G.; Malrieu, J. P. *J. Am. Chem. Soc.* **1987**, *109*, 5303; *J. Phys. Chem.* **1990**, *94*, 6184. Trinquier, G. *J. Am. Chem. Soc.* **1990**, *112*, 2130.

(24) Liang, C.; Allen, L. C. *J. Am. Chem. Soc.* **1990**, *112*, 1039.

(25) Grev, R. S.; Schaefer, H. F., III.; Baines, K. M. *J. Am. Chem. Soc.* **1990**, *112*, 9458.

(26) Colegrove, B. T.; Schaefer, H. F. III. *J. Phys. Chem.* **1990**, *94*, 5593.

(27) Curtiss, L. A.; Raghavachari, K.; Deutsch, P. W.; Pople, J. A. *J. Chem. Phys.* **1991**, *95*, 2433.

(28) Grev, R. S.; Schaefer, H. F. III. *J. Chem. Phys.* **1992**, *97*, 7990.

(29) Kalcher, J.; Sax, A. F. *Chem. Phys. Lett.* **1992**, *192*, 451.

(30) Hühn, M. M.; Amos, R. D.; Kobayashi, R.; Handy, N. C. *J. Chem. Phys.* **1993**, *98*, 7107.

(31) Ernst, M. C.; Sax, A. F.; Kalcher, J. *Chem. Phys. Lett.* **1993**, *216*, 189.

(32) Jacobsen, H.; Ziegler, T. *J. Am. Chem. Soc.* **1994**, *116*, 3667 and references therein.

(33) Pak, C.; Rienstra-Kiracofe, J. C.; Schaefer, H. F., III. *J. Phys. Chem. A* **2000**, *104*, 11232 and references therein.

(34) Maier, G.; Mihm, G.; Reisenauer, H. P. *Angew. Chem.* **1981**, *93*, 615; *Angew. Chem., Int. Ed. Engl.* **1981**, *20*, 597.

(35) Bailleux, S.; Bogey, M.; Demaison, J.; Bürger, H.; Senzlober, M.; Breidung, J.; Thiel, W.; Fajgar, R.; Pola, J. *J. Chem. Phys.* **1997**, *106*, 10016.

(36) Bogey, M.; Bolvin, H.; Demuynck, C.; Destombes, J. L. *Phys. Rev. Lett.* **1991**, *66*, 413.

(37) Cordonnier, M.; Bogey, M.; Demuynck, C.; Destombes, J.-L. *J. Chem. Phys.* **1992**, *97*, 7984.

(38) Ruscic, B.; Berkowitz, J. *J. Chem. Phys.* **1991**, *95*, 2416.

(39) Tonokura, K.; Murasaki, T.; Koshi, M. *Chem. Phys. Lett.* **2000**, *319*, 507.

(40) Chambreau, S. D.; Zhang, J. S. *Chem. Phys. Lett.* **2001**, *343*, 482.

(41) Tada, N.; Tonokura, K.; Matsumoto, K.; Koshi, M.; Miyoshi, A.; Matsui, H. *J. Phys. Chem. A* **1999**, *103*, 322.

(42) Burger, H.; Eujen, R. Z. *Naturforsch. B: Anorg. Chem., Org. Chem.* **1974**, *29*, 647.

(43) Reed, K. J.; Brauman, J. I. *J. Chem. Phys.* **1974**, *61*, 4830.

(44) Sheldon, J. C.; Bowie, J. H.; DePuy, C. H.; Dramrauer, R. *J. Am. Chem. Soc.* **1986**, *108*, 6794.

(45) Nimlos, M. R.; Ellison, G. B. *J. Am. Chem. Soc.* **1986**, *108*, 6522.

(46) Shen, M.; Schaefer, H. F., III. *Mol. Phys.* **1992**, *76*, 467.

(47) Kirsten, A.; Császár, A. G.; Sibert, E. L., III.; Allen, W. D.; Schaefer, H. F., III.; Klopper, W.; Noga, J. *J. Chem. Phys.* **2000**, *112*, 4053.

(48) Spirko, V.; Kraemer, W. P. *J. Mol. Struct. (THEOCHEM)* **2001**, *547*, 139.

(49) Burkholder, T. R.; Andrews, L. *J. Chem. Phys.* **1991**, *95*, 8697.

(50) Hassanzadeh, P.; Andrews, L. *J. Phys. Chem.* **1992**, *96*, 9177.

(51) Frisch, M. J.; Trucks, G. W.; Schlegel, H. B.; Scuseria, G. E.; Robb, M. A.; Cheeseman, J. R.; Zakrzewski, V. G.; Montgomery, J. A., Jr.; Stratmann, R. E.; Burant, J. C.; Dapprich, S.; Millam, J. M.; Daniels, A. D.; Kudin, K. N.; Strain, M. C.; Farkas, O.; Tomasi, J.; Barone, V.; Cossi, M.; Cammi, R.; Mennucci, B.; Pomelli, C.; Adamo, C.; Clifford, S.; Ochterski, J.; Petersson, G. A.; Ayala, P. Y.; Cui, Q.; Morokuma, K.; Malick, D. K.; Rabuck, A. D.; Raghavachari, K.; Foresman, J. B.; Cioslowski, J.; Ortiz, J. V.; Baboul, A. G.; Stefanov, B. B.; Liu, G.; Liashenko, A.; Piskorz, P.; Komaromi, I.; Gomperts, R.; Martin, R. L.; Fox, D. J.; Keith, T.; Al-Laham, M. A.; Peng, C. Y.; Nanayakkara, A.; Gonzalez, C.; Challacombe, M.; Gill, P. M. W.; Johnson, B.; Chen, W.; Wong, M. W.; Andres, J. L.; Gonzalez, C.; Head-Gordon, M.; Replogle, E. S.; Pople, J. A. *Gaussian 98*, revision A.7; Gaussian, Inc.: Pittsburgh, PA, 1998.

(52) (a) Becke, A. D. *J. Chem. Phys.* **1993**, **98**, 5648. (b) Lee, C.; Yang, W.; Parr, R. G. *Phys. Rev. B* **1988**, *37*, 785.

(53) (a) Becke, A. D. *Phys. Rev. A* **1988**, *38*, 3098. (b) Perdew, J. P.; Wang, Y. *Phys. Rev. B* **1992**, *45*, 13244.

(54) (a) Krishnan, R.; Binkley, J. S.; Seeger, R.; Pople, J. A. *J. Chem. Phys.* **1980**, *72*, 650. (b) Frisch, M. J.; Pople, J. A.; Binkley, J. S. *J. Chem. Phys.* **1984**, *80*, 3265.

(55) Jacox, M. E. *Chem. Phys.* **1994**, *189*, 149.

(56) Zhou, M. F.; Andrews, L. *J. Am. Chem. Soc.* **1998**, *120*, 11499.

(57) Zhou, M. F.; Andrews, L. *J. Chem. Phys.* **1999**, *110*, 2414.

(58) Zhou, M. F.; Andrews, L. *J. Phys. Chem. A* **2000**, *104*, 3914.

(59) Kasdan, A.; Herbst, E.; Lineberger, W. C. *J. Chem. Phys.* **1975**, *62*, 541.

(60) Huber, K. P.; Herzberg, G. *Molecular Spectra and Molecular Structure. IV. Constants of Diatomic Molecules*; Van Nostrand Reinhold: New York, 1979.

(61) (a) Milligan, D. E.; Jacox, M. E. *J. Mol. Spectrosc.* **1973**, *46*, 460. (b) Wight, C. A.; Ault, B. S.; Andrews, L. *J. Chem. Phys*. **1976**, *65*, 1244.

(62) Knight, L. B., Jr.; Winiski, M.; Kudelko, P.; Arrington, C. A. *J. Chem. Phys.* **1989**, *91*, 3368.

(63) Zhang, L.; Dong, J.; Zhou, M. F. *J. Chem. Phys*. **2000**, *113*, 8700.

(64) Kang, H.; Beauchamp, J. L. *J. Phys. Chem*. **1985**, *89*, 3364.

(65) Berkowitz, J.; Greene, J. P.; Cho, H.; Ruscic, B. *J. Chem. Phys.* **1987**, *86*, 1235.

(66) (a) Milligan, D. E.; Jacox, M. E. *J. Chem. Phys.* **1963**, *38*, 2627. (b) Smith, D. W.; Andrews, L. *J. Chem. Phys.* **1974**, *60*, 81.

(67) Zhou, M. F.; Andrews, L.; Bauschlicher, C. W., Jr. *Chem. Rev.* **2001**, *101*, 1931.